2-(4-fluorobenzyl) chromeno [2,3-c] pyrozol-3(2H)-one as copper corrosion inhibitor in HNO_3 : gravimetric and quantum chemical investigation methods

ABSTRACT

The use of organic compounds as corrosion inhibitors has become a principal means of protecting metal equipment in industrial applications. This work therefore set out to evaluate the inhibiting properties of 2-(4-fluorobenzyl) chromeno [2,3-c] pyrozol-3(2H)-one for copper corrosion in 1M nitric acid solution. These properties were investigated using gravimetric method and quantum chemical calculations. Inhibition efficiency increased with temperature, inhibitor concentration and immersion time. Adsorption of this molecule on copper surface occurs according to Langmuir isotherm, while the thermodynamic parameters of absorption and kinetics prove that adsorption is spontaneous and dominated by chemisorption. Quantum chemical parameters derived from density functional theory (DFT) revealed that there is a strong interaction based on electronic exchange between the inhibitor and copper.

Keywords: [2-(4-fluorobenzyl) chromeno [2,3-c] pyrozol-3(2H)-one, Gravimetric method , quantum chemical calculations, Copper corrosion , Nitric acid

1. INTRODUCTION

The need to find inexpensive, non-toxic and effective corrosion inhibitors has become a concern in industrial sector [1,2]. Indeed, metal destruction during acid pickling operations leads to high maintenance costs in many companies [3,4].These maintenance costs often extend to the replacement of corroded metal equipment. In addition, copper's good electrical and thermal conductivity and ease of soldering make it widely used in industry, construction, electrical installations and water pipes [5]. Use of corrosion inhibitors is a means of protecting these metal equipment to ensure their longevity [6,7]. Corrosion inhibitors must be added in low concentrations to corrosive media [8]. Their role is to modify the corrosive environment in which pickling operations take place, making them less corrosive. This modification helps to reduce metal dissolution in the medium. However, the application time, cost and toxic nature of certain compounds limit their use [9]. Several organic and inorganic compounds have been studied as inhibitors [10,11]. But recent research suggests that organic compounds with heteroatoms in their structure, such as nitrogen, sulfur, oxygen, phosphorus and aromatic rings with π-bonds, may retard copper dissolution during acid pickling operations [12-14]. Computational chemistry based on density functional theory calculations has shown in recent years that the inhibition activity of these organic compounds depends on the heteroatoms and π-bonds present in their molecular structure [15-17]. In fact, experimental methods indicate protection but do not explain the protection procedure. In a bid to explain the inhibition mechanism, DFT method has recently been called upon for its high degree of accuracy. This method permits to establish a satisfactory

correlation between the molecular properties of inhibitors and their corrosion-inhibiting efficiency.
The aim of the present study is to establish a correlation between the theoretical molecular properties of 2-(4-fluorobenzyl) chromeno [2,3-c] pyrozol-3(2H)-one and its experimental inhibition activity in copper corrosion in 1M HNO_3 medium. The molecular structure of this compound is shown in Fig. 1.

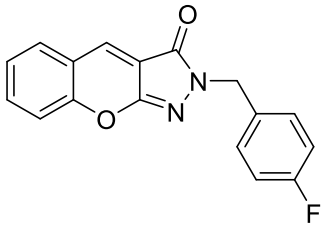

Fig 1: Molecular structure of 2-(4-fluorobenzyl) chromeno [2,3-c] pyrozol-3(2H)-one (FCP)

2. EXPERIMENTAL TECHNIQUES

2.1 Mass Loss Method

Experimental technique used in this work is mass loss. This technique involves soaking a copper sample in nitric acid for a given period of time.
Using commercial acid with the following characteristics: purity, P = 69%, density, d=1.41 and molar mass M = 63, 01 $g.mol^{-1}$. A 1M blank solution was prepared from this commercial solution. From FCP powder, four concentrations of 0.08mM; 0.15mM; 0.3mM and 0.6mM were prepared using 1M nitric acid as the blank solution.
Copper samples of 99.6% purity, cylindrical in shape, 1cm length and 0.25cm in diameter, were first polished with 100 to 1200 grit abrasive paper. They were then rinsed with distilled water and washed in an acetone solution. An oven maintained at a temperature of 80°C was used to dry the samples for 20 minutes. On removal from the oven, each sample was weighed (m_1) using a precision balance: ± 0.1 mg. Each sample is then immersed in 50 ml of 1M nitric acid corrosive solution with or without FCP inhibitor. After two hours of immersion at a constant temperature in a thermostated bath, each sample is removed from the solution, rinsed thoroughly with distilled water, dried and then reweighed (m_2). The different temperatures set during the experiment range from 298K to 338K.
The quantities that are Corrosion rate (W), the rate of surface coverage (θ) and the inhibition efficiency (IE) were calculated from the expressions below [18,19]:

$$W = \frac{m_1 - m_2}{s.t} \quad (1)$$

$$\theta = \frac{W_0 - W}{W_0} \quad (2)$$

$$IE(\%) = \frac{W_0 - W}{W_0} * 100 \quad (3)$$

W_0 and W; are respectively copper corrosion rate in absence and presence of FCP

2.2 Theoretical calculations

The theoretical approach used was density functional theory (DFT). This theory was used to explain FCP inhibition activity on copper surface. DFT calculations were performed using Gaussian-09 program [20]. Exchange correlation was performed using B3LYP hybrid functionals (three-parameter Beckes with Lee-Yang-Parr hybrid correlation functional) combined with the 6-31G (d,p) basis set [21,22]. The molecular structure was geometrically optimized using this functional and in 6-31G (d,p) basis set. All these calculations were performed in gas and aqueous phase. All these calculations were carried out in the gas and

aqueous phases. Consequently, the parameters that describe global reactivity, such as highest occupied molecular orbital energy (EHOMO), lowest unoccupied molecular orbital energy (ELUMO), energy gap (ΔE), dipole moment (μ), total energy (ET), electron affinity (*A*), the ionization energy (*I*), electronegativity (χ), hardness (η), softness (σ) and electrophylicity index (ω), fraction of electrons transferred (ΔN) and electron acceptor (ω^+) and electron donor (ω^-) indices have been deduced from E_{HO} and E_{BV}. Local reactivity parameters such as Fukui functions and the dual descriptor were calculated in order to identify likely attack sites.

3. RESULTS AND DISCUSSION

3.1 Experimental results analysis

3.1.1 Combined effect of temperature and concentration on inhibition efficiency

The combined effect of temperature and concentration on inhibition efficiency (IE) is shown in Fig. 2.

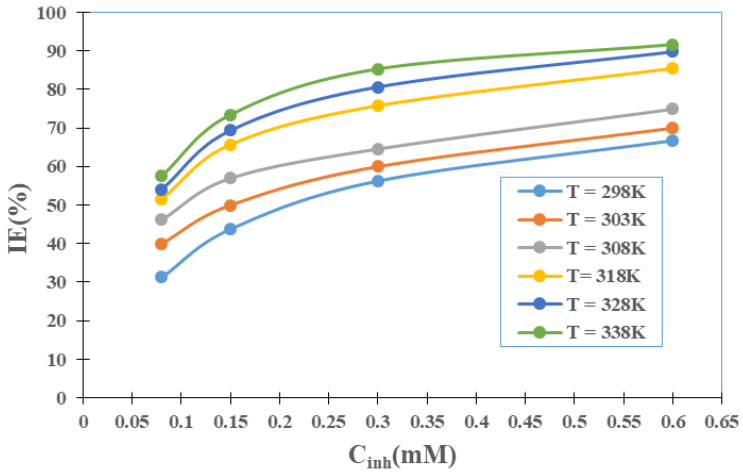

Fig 2: Effect of temperature and concentration on FCP inhibition efficiency

Fig. 2 examination reports that FCP inhibition efficiency (IE) increases with increasing reaction medium temperature and inhibitor concentration. These observations mentions that metal surface coating thickens as FCP concentration and temperature evolve. This coating, which results from the formation of a complex between FCP and metal, is deposited more and more on copper surface to reduce its dissolution as temperature and concentration increase. These data reveal that the combined action of temperature and concentration describes the evolution of the inhibition efficiency of the compound studied. Similar reports were found in the literature [23,24].

3.1.2 Immersion time effect

Immersion time effect is described by Fig.3, which indicates that FCP inhibition efficiency increases with immersion time. In fact, for a given temperature, FCP inhibition efficiency of 6h immersion time is higher than that of 4h, 2h and 1h immersion times. These results certify that the layer that attaches to metal surface becomes more compact with increasing time

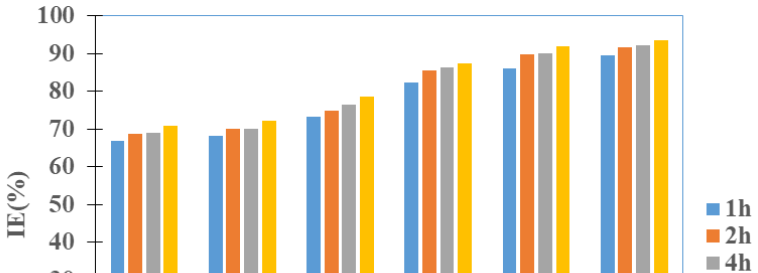

and temperature. In this case, FCP is able to provide protection as time and temperature increase.

Fig 3. Effect of immersion time on inhibition efficiency

3.1.3 Activation kinetic parameters

Temperature influence on the corrosion process provides access to the activation parameters. The dependence of the corrosion rate on the temperature of reaction medium is defined by Arrhenius relation. This relationship, expressed as follows, enables us to calculate the activation energy (E_a) [25].

$$W = Aexp(-\frac{E_a}{RT}) \quad (4)$$

As for the alternative formula of Arrhenius equation, it allows us to determine the activation enthalpy (ΔH_a^*) and the activation entropy (ΔS_a^*). Its expression is as follows [24]:

$$W = \frac{RT}{N_A h} exp\left(\frac{\Delta S_a^*}{R}\right).exp\left(-\frac{\Delta H_a^*}{R.T}\right) \quad (5)$$

Where: A is the frequency factor, R is the universal gas constant, T is the absolute temperature, N_A: Avogadro number , h : Planck's constant.
Fig. 4 shows the activation energy, while Fig. 5 shows the enthalpy (ΔH_a^*) and activation entropy(ΔS_a^*).

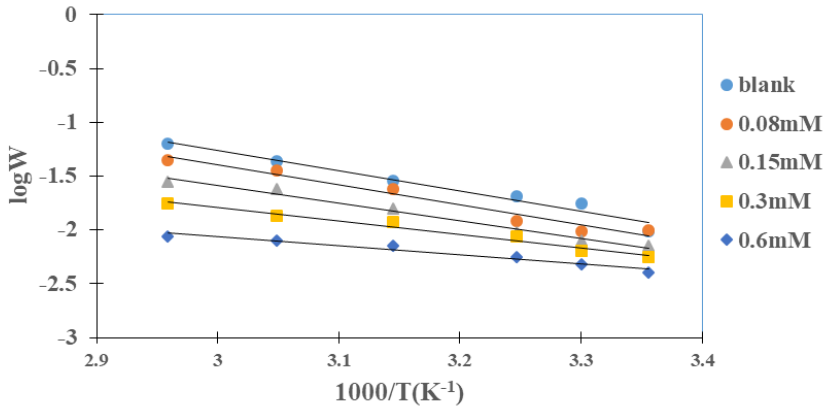

Fig 4. LogW versus $\frac{1}{T}$

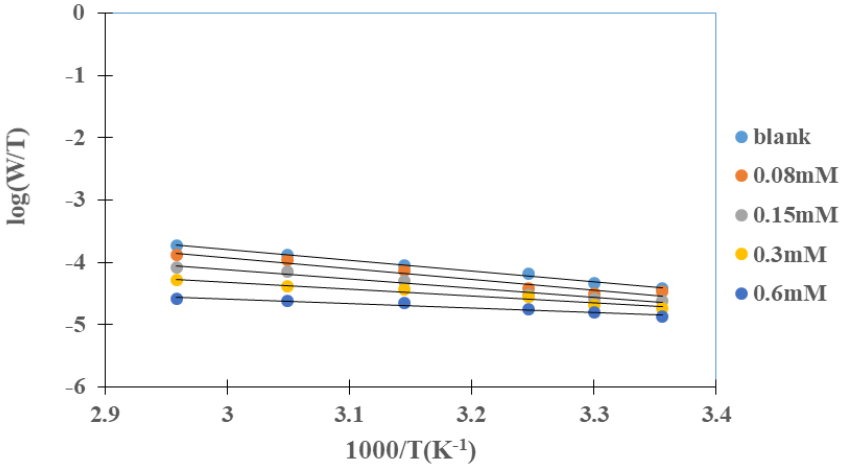

Fig. 5. Log($\frac{W}{T}$) versus $\frac{1}{T}$

The values of these different activation parameters are given in Table 1.

Table 1. Activation parameters

C_{inh} (mM)	E_a (kJ.mol^{-1})	ΔS_a^* (J.mol^{-1} K^{-1})	ΔH_a^* (kJ.mol^{-1})	$E_a - \Delta H_a^*$ ($kJmol^{-1}$)
0	35.96	-170.16	33.33	2.63
0.08	35.68	-173.65	33.00	2.68
0.15	31.19	-190.58	28.55	2.63
0.3	23.89	-216.33	21.26	2.63
0.6	16.41	-243.97	13.77	2.64

Activation energy (E_a) in FCP absence is higher than E_a values in FCP presence. This drop in activation energy in FCP presence confirms the formation of Cu-inh complex on metal surface. These data reveal that FCP addition in corrosive medium promotes the reduction of copper corrosion in the said medium [26].

Table 1 inspection reveals that ΔH_a^* values are positive, indicating that copper dissolution process is endothermic. The negative values of ΔS_a^* which decrease as FCP concentration increases mention that the complex formation reduces the disorder created by water molecules desorption [25]. The difference in $E_a - \Delta H_a^*$ is constant for all concentrations, revealing that E_a and ΔH_a^* vary in the same way suggests that copper dissolution process and adsorption occur on surface and this adsorption is dominated by chemisorption [27].

3.1.4 Thermodynamic adsorption parameters

FCP adsorption properties on copper surface were described by thermodynamic adsorption parameters. These parameters were deduced from a suitable adsorption model.

The search for a suitable model was carried out by fitting experimental results to several models including Temkin, El-Awady, Langmuir and Freundlich. Langmuir model is the most appropriate, as it has correlation coefficients closer to unity. The expression of this isotherm is written as follows [28]:

$$\frac{C_{inh}}{\theta} = \frac{1}{K_{ads}} + C_{inh} \qquad (6)$$

Fig. 6 illustrates this isotherm.

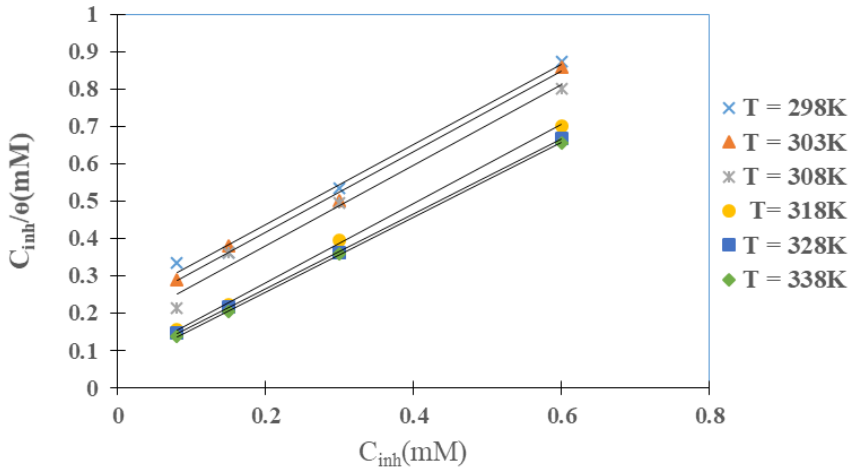

Fig. 6. Langmuir isotherm representation

This model states that FCP adsorbs to copper surface by a single layer and interactions between adsorbed particles are negligible [28]. Adsorption parameters such as: standard free adsorption enthalpy(ΔG^0_{ads}), standard adsorption enthalpy (ΔH^0_{ads}) and standard adsorption entropy (ΔS^0_{ads}) are calculated from the adsorption equilibrium constant. The following expressions are used to calculate these quantities [29]:

$$\Delta G^0_{ads} = -RTln(55.5K_{ads}) \qquad (7)$$

$$\Delta G^0_{ads} = \Delta H^0_{ads} - T\Delta S^0_{ads} \qquad (8)$$

- R : Universal gas constant ;
- T : Absolute temperature ;
- 55.5: the concentration of water (in mol/L) in the solution.
- K_{ads} Values (adsorption equilibrium constant) are deduced from the equations of the straight lines obtained from the Langmuir isotherm.

The intercept and the slope of the straight line obtained in Fig. 7 give ΔS^0_{ads} and ΔH^0_{ads} values respectively. The various values of these Thermodynamic Adsorption Parameters are listed in Table 2.

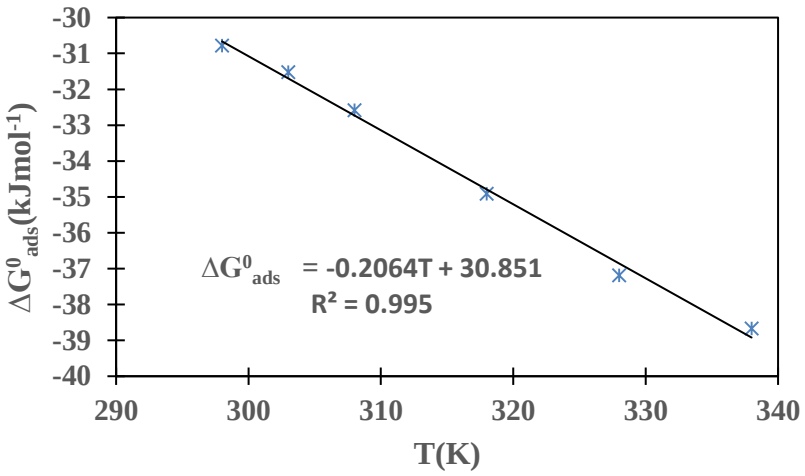

Fig 7. ΔG^0_{ads} versus température

Table 2. Thermodynamique adsorption parameter values

T(K)	K_{ads} (M^{-1})	ΔG^0_{ads} $(kJ\ mol^{-1})$	ΔH^0_{ads} $(kJ\ mol^{-1})$	ΔS^0_{ads} $(J\ mol^{-1}K^{-1})$
298	4446.42	-30.78		
303	4928.54	-31.52		
308	6082.73	-32.58	30.85	206.4
318	14388.49	-35.91		
328	15174.51	-37.19		
338	17182.13	-38.67		

Table 2 Analysis indicates that K_{ads} values are high, indicating a strong FCP adsorption on copper surface [17]. Which adsorption confirms the good inhibition performance obtained experimentally. ΔG^0_{ads} .Values obtained suggest that both chemical and physical adsorption are involved in FCP action on copper surface [30,31]. This adsorption is spontaneous and promotes a stable layer. ΔH^0_{ads} positive values denote that the process of setting up this layer is endothermic [32]. The increase in disorder during the process of FCP adsorption on copper is evidenced by the positive ΔS^0_{ads} value. This disorder results from water molecules desorption on copper surface [32].

3.2 Correlating experimental and theoretical data

The optimized structures of neutral (FCP) and protonated (FCPH+) forms are shown in Fig. 8.

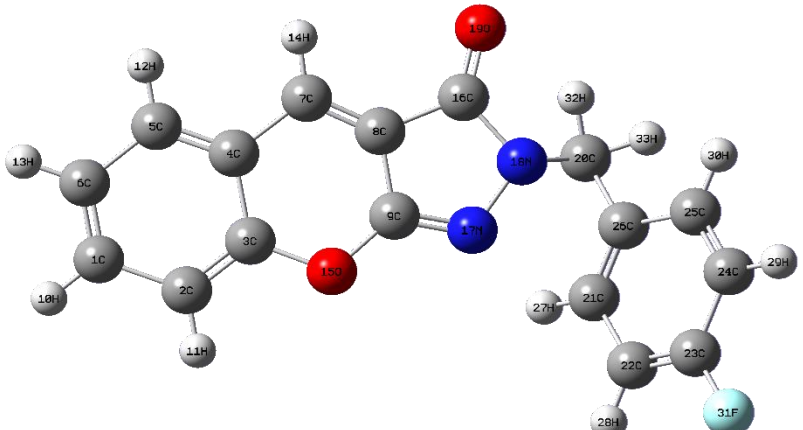

(a)

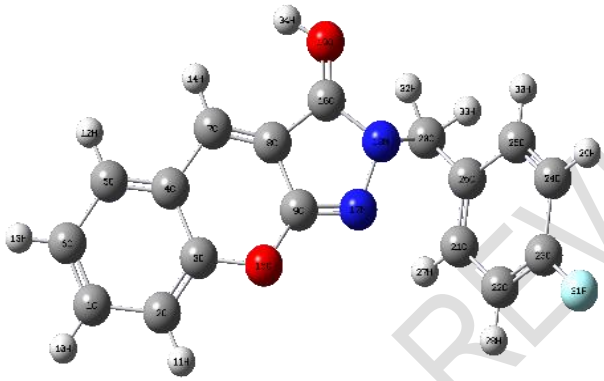

(b)

Fig. 8. Optimized structure of FCP(a) and FCPH+ (b)

The quantum chemical parameters obtained from B3LYP functional and in 6-31G(d,p) basis set are reported in Table 3.

Table 3. Global reactivity parameters of neutral FCP and its protonated form

Quantum chemical parameters	FCP	$FCPH^+$
E_{HOMO} (eV)	-5.7199	-5.6923
E_{LUMO} (eV)	-2.6738	-2.7179
Energy gap ΔE (eV)	3.0461	2.9744
Dipole moment μ (D)	5.2806	5.9578
Ionization energy I (eV)	5.7199	5.6923
Electron affinity A (eV)	2.6738	2.7179
Electronegativity χ (eV)	4.1969	4.2051
Hardness η (eV)	1.5230	1.4872
Softness (σ) $(eV)^{-1}$	0.6566	0.6724
Fraction of electron transferred ΔN	0.2571	0.2605
Electrophylicity index ω	5.7824	5.9450

Electroaccepting power ω^+	3.8742	4.0284
Electrodonating power ω^-	8.0711	8.2335
Total energy E_T (Ha)	-1013.9580	-1014.6734

Quantum chemical parameters derived from DFT calculations help explain the relationship between the inhibition efficiency of an inhibitor and its electronic structure [33].

Indeed, the high value of E_{HOMO} obtained suggests a high capacity of FCP to donate electrons to metal, which is a suitable receptor. On the other hand, the low value of E_{LUMO} obtained stipulates that FCP can receive electrons from the metal [34,35]. Furthermore, the energy difference between LUMO and HOMO (ΔE = E_{LUMO} - E_{HOMO}) called energy gap is a factor that informs about the reactivity of a molecule [36]. In this study ΔE is lower, justifying the good inhibition performance of FCP obtained experimentally.

The organic compound studied contains isolated electron pairs of oxygen (O) and nitrogen (N) atoms in its structure. Thus the molecule can donate electrons to the vacant low-energy d orbital including Cu^{2+} ions. Copper metal in an acidic medium oxidizes and releases electrons to the molecule. This process of electron donation and acceptance promotes the formation of a Cu-FCP complex on metal surface. This complex reduces metal corrosion.

FCP dipole moment (μ) increases with its protonated form, in which case the molecule adsorbs more strongly to copper surface [37].

The ionization potential (*I*) and electronic affinity (*A*) are obtained from the following relationships [38]:

$$I = -E_{HOMO} \quad (9)$$

$$A = -E_{LUMO} \quad (10)$$

The magnitude values *I* and A indicate FCP is capable of giving and receiving electrons from copper.

As for softness (σ) and global hardness (η) obtained using the following relationships respectively [38]:

$$\eta = \frac{I-A}{2} \quad (11)$$

$$\sigma = \frac{1}{\eta} = \frac{2}{I-A} \quad (12)$$

These values mention that the molecule has a high softness value and a low hardness value. These results confirm that the molecule is highly reactive and can easily donate electrons to copper. Which reactivity justifies the good experimental values.

Parameters such as the electronegativity (χ) of FCP and the Fraction of electron transferred (ΔN) are expressed as follows [39]:

$$\chi = \frac{I+A}{2} \quad (13)$$

$$\Delta N = \frac{\chi_{cu} - \chi_{inh}}{2(\eta_{cu} + \eta_{inh})} \qquad (14)$$

The calculations were performed using the following theoretical values:

$\chi_{cu} = 4.98\ eV$ [40] et $\eta_{cu} = 0$ [40].

Copper electronegativity (4.98 eV) is greater than that of the neutral molecule (4.1969 eV) and of the protonated form (4.2051). In this case, the electron-attracting effect of copper is higher than that of FCP. Then FCP electrons are therefore attracted to copper. Moreover, the fraction of electrons transferred is greater than zero (ΔN >0), confirming the flow of electrons from FCP to copper. This movement of electrons towards copper leads to the formation of covalent bonds. These bonds enable the compound to bind easily to the metal surface.

The electrophilicity index (ω) can be calculated using the following expression [41]:

$$\omega = \frac{\mu_P^2}{2\eta} = \frac{(\mathrm{I+A})^2}{4(\mathrm{I-A})} \qquad (15)$$

The electron acceptor (ω^+) and electron donor (ω^-) indices are respectively calculated from the following relationships [41,42]:

$$\omega^+ = \frac{(I+3A)^2}{16(I-A)} \qquad (16)$$

$$\omega^- = \frac{(3I+A)^2}{16(I-A)} \qquad (17)$$

The ability of an organic compound to donate or receive electrons also depends on its electrophilicity index. In this study, the high value of ω attests that FCP is a good electrophile and has a good capacity to accept electrons from copper [43]. Furthermore, we observe that $\frac{\omega^+ + \omega^-}{2} \approx E_{HO}$ for both forms, revealing that FCP possesses a good ability to donate electrons to copper.

The good inhibition capacity obtained experimentally is based on the donor and acceptor abilities possessed by the molecule studied. Which molecule is more reactive on its protonated form.

3.2 FCP electron gain and loss sites

The molecule gains electrons from LUMO orbital (Fig 9) and loses electrons from HOMO orbital. The parameters that identify these sites of reactivity are the Fukui functions (f_k^+ , f_k^-) and dual descriptor ($\Delta f_k(\mathrm{r})$.These local quantities are expressed as follows [44]:

- Nucléophilic attack $f_k^+ = q_k(N+1) - q_k(N)$ (18)
- Electrophilic attack $f_k^- = q_k(N) - q_k(N-1)$ (19)

Where $q_k(N+1)$, $q_k(N)$ et $q_k(N-1)$ are the electronic population of atom k in $(N+1)$, N and $(N-1)$ electrons systems. N is the number of electrons in the neutral species,when $(N+1)$ corresponds to an anion with an electron added to LUMO of molecule and $(N-1)$ is the cation with an electron removed from HOMO molecule.

Dual descriptor ($\Delta f_k(\mathrm{r})$ is expressed as follows [45,46]:

$$\Delta f_k(\mathrm{r}) = f_k^+ - f_k^- \qquad (27)$$

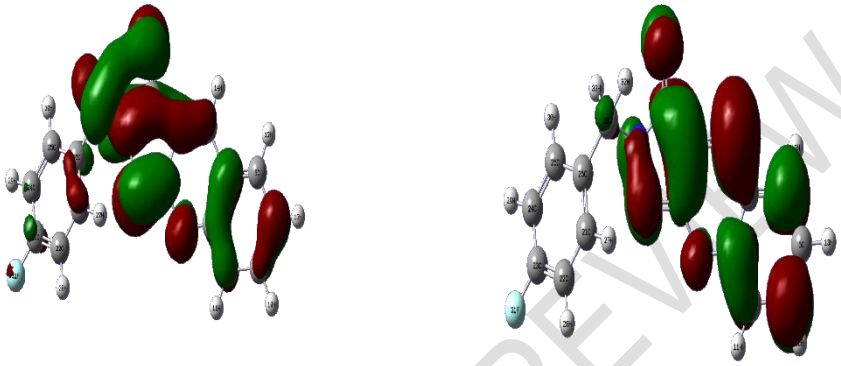

Orbital HOMO Orbital LUMO

Fig 9. HOMO and LUMO orbitals

Table 4 presents the values of Mulliken charges, the Fukui functions and the dual descriptor.

Table 4. Local reactivity parameters

atoms	$q_k(N+1)$	$q_k(N)$	$q_k(N-1)$	f_k^+	f_k^-	$\Delta f_k(\mathrm{r})$
1 C	-0.004173	0.076223	0.136997	-0.080396	-0.060774	-0.019622
2 C	0.00616	-0.159769	-0.033103	0.165929	-0.126666	0.292595
3 C	-0.003792	0.340401	0.044013	-0.344193	0.296388	-0.640581
4 C	0.001878	0.073372	-0.070648	-0.071494	0.14402	-0.215514
5 C	-0.002965	-0.153374	0.190708	0.150409	-0.344082	0.494491
6 C	0.003624	-0.088499	-0.072346	0.092123	-0.016153	0.108276

7	C	-0.007188	-0.101043	0.41632	0.093855	-0.517363	0.611218
8	C	-0.002245	-0.003098	0.025972	0.000853	-0.02907	0.029923
9	C	0.026392	0.580425	0.021723	-0.554033	**0.558702**	**-1.112735**
10	H	0.000151	0.110618	-0.00695	-0.110467	0.117568	-0.228035
11	H	-0.000256	0.12029	0.000969	-0.120546	0.119321	-0.239867
12	H	0.000127	0.111545	-0.008887	-0.111418	0.120432	-0.23185
13	H	-0.000148	0.105153	0.002465	-0.105301	0.102688	-0.207989
14	H	0.000242	0.13806	-0.018857	-0.137818	0.156917	-0.294735
15	O	0.010827	-0.559941	0.014555	0.570768	-0.574496	1.145264
16	C	0.00252	0.573488	0.151196	-0.570968	0.422292	-0.99326
17	N	0.009915	-0.346909	0.090696	0.356824	-0.437605	0.794429
18	N	0.128765	-0.346227	-0.024047	0.474992	-0.32218	0.797172
19	O	0.021922	-0.508647	0.118353	0.530569	-0.627	1.157569
20	C	0.781676	-0.322163	0.028442	**1.103839**	-0.350605	**1.454444**
21	C	0.022046	-0.017681	-0.001296	0.039727	-0.016385	0.056112
22	C	-0.006078	-0.159432	-0.000736	0.153354	-0.158696	0.31205
23	C	0.007757	0.337906	-0.000083	-0.330149	0.337989	-0.668138
24	C	0.020226	-0.143659	-0.001074	0.163885	-0.142585	0.30647
25	C	0.012082	-0.084937	0.000672	0.097019	-0.085609	0.182628
26	C	-0.01275	-0.030656	0.001452	0.017906	-0.032108	0.050014
27	H	0.001417	0.129814	0.000071	-0.128397	0.129743	-0.25814
28	H	0.000488	0.100229	-0.000099	-0.099741	0.100328	-0.200069
29	H	0.000838	0.098956	0.000301	-0.098118	0.098655	-0.196773
30	H	-0.000369	0.091602	-0.00022	-0.091971	0.091822	-0.183793
31	F	0.001679	-0.291247	0.000006	0.292926	-0.291253	0.584179
32	H	-0.015552	0.223437	0.00175	-0.238989	0.221687	-0.460676
33	H	-0.005214	0.258209	-0.008315	-0.263423	0.266524	-0.529947

Table 3 analysis indicates that carbon C(9) has the highest value of f_k^- and the lowest value of $\Delta f_k(\mathrm{r})$.This atom represents the probable site for receiving electrophilic attacks. The probable site for receiving nucleophilic attacks is governed by atom C(20), which has the highest values of f_k^+ and $\Delta f_k(\mathrm{r})$. The molecule could receive electrons from Cu^{2+} ions at C(20) center belonging to LUMO zone. It could also donate electrons to the unoccupied copper d orbital through C(9) atom, center belonging to HOMO zone. These exchanges reinforce the interactions between copper and FCP, resulting in the formation of a physical barrier (Cu-FCP) that prevents direct contact between the metal and the corrosive medium [46].

CONCLUSION

This work led to the following conclusions:

- ❖ FCP exhibits good inhibition of copper corrosion in 1M nitric acid. Its inhibition efficiency increasing with concentration, reaction medium temperature and immersion time.
- ❖ Activation kinetics parameters reveal the formation of a Cu-FCP complex on copper surface. This complex reduces copper dissolution in the medium studied.
- ❖ The difference in $E_a - \Delta H_a^*$ is constant, indicating a surface adsorption reaction dominated by chemical adsorption.
- ❖ This surface adsorption is consistent with Langmuir isotherm model. It is spontaneous, endothermic and increases disorder.
- ❖ Quantum parameters calculated using DFT reveal that FCP inhibition performance obtained by gravimetric tests is due to electron exchange between FCP molecule and copper. The carbons C(9) and C(20) are responsible for these electron exchanges. The protonated form of the molecule is the most reactive.
- ❖ Finally, there is good agreement between experimental and theoretical data.

REFERENCES

1. Glaydson LFM, Stefane NC, Valder NF, Paulo NSC, Adriana NC, Pedro de LN.Understanding the corrosion inhibition of carbon steel and copper in sulphuric acid medium by amino acids using electrochemical techniques allied to molecular modelling methods. Corrosion Science. 2017; 115: 41-55.

2. Nataša K, Ingrid M, Anton K. How relevant is the adsorption bonding of imidazoles and triazoles for their corrosion inhibition of copper? Corrosion Science.2017; 124:25-34.

3. Changming B, Xiang G, Kanglu F, Juan Q, Kangwei G, Chunchao C, Houyi M. Effect of Sn on the micro-structure, composition and anti-corrosion performance of reduced glutathione film on copper. Colloids and Surfaces A: Physicochemical and Engineering Aspects. 2024; 692: 133954.

4. Jie Z, Yue G, Zhixiong X, Hanhong Z, Bochuan T, Wenpo L. Adsorption films based on indazole derivatives for application to protect Cu in sulfuric acid: Experimental and theoretical approaches.Journal of the Taiwan Institute of Chemical Engineers. 2023; 151: 105134.

5. Xiaomeng S., Jian P., Yujie Q., Yue Z., Song Z. Recent advances in protective technologies against copper corrosion. Journal of Materials Science & Technology. 2024; 201: 75-94.

6. Dahmani K, Galai M, Ouakki M, Elgendy A, Ez-Zriouli R, Lachhab R, Briche S, Cherkaoui M. Corrosion inhibition of copper in sulfuric acid via environmentally friendly inhibitor (Myrtus Communis): Combining experimental and theoretical methods. Journal of Molecular Liquids. 2022, 347:117982.

7. Ping H, Pengliang C, Yundong W, Lei G, Abeer AA. Insight into the corrosion inhibition performance of Capsicum annuum L. leaf extract as corrosion inhibitor for copper in sulfuric acid medium. Journal of the Taiwan Institute of Chemical Engineers. 2024; 161: 105558.

8. Oubahou M, El aloua A, Benzbiria N, El Harrari S, Takky D, Naimi Y, Zeroual A, Shifa W, Syed A, Belghiti ME. Electrochemical, thermodynamic and computational investigation of the use of an expired drug as a sustainable corrosion inhibitor for copper in 0.5 M H_2SO_4. Materials Chemistry and Physics. 2024; 323:129642.

9. Wenpo L., Wei L., Xinke Y., Chaowei M., Yan X, Bochuan T, Yujie Q. Adsorption and inhibition behavior of 3-chloro-6-mercaptopyridazine towards copper corrosion in sulfuric acid. Journal of Molecular Liquids. 2022; 357:119100.

10. Mourad R, Omar D, Rachid H., Hasnaa H, Zaki SS, Mariya K, Hansang K, Avni B, Nuha AW, Ohoud SA, Elyor B, Mohamed R, Mohcine S, Ilyos E. New triglycidyl ether triazine as a protective agent for metal: Comprehensive analysis. Materials Chemistry and Physics. 2024, 327: 129907.

11. Zhifeng H, Xia H, Jiachang C., Junying C., Herong Z. Study on the compounding of cysteine modified Schiff base and decanoic acid as corrosion inhibitors for bronze with patina,Surfaces and Interfaces. 2024; 46:103996.

12. Ling Z, Shengtao Z, Bochuan T, Li F, Bin X, Feng C, Weining L, Bingxue X, Tingting S.Phenothiazine drugs as novel and eco-friendly corrosion inhibitors for copper in sulfuric acid solution. Journal of the Taiwan Institute of Chemical Engineers. 2020; 113: 253-263.

13. Bochuan T, Shengtao Z, Xianlong C, Anqing F, Lei G, Riadh M, Wenpo L. Insight into the anti-corrosion performance of two food flavors as eco-friendly and ultra-high performance inhibitors for copper in sulfuric acid medium. Journal of Colloid and Interface Science. 2022; 609: 838-851.

14. Khaled M. A., Ismail M. A., Ahmed. A. El-Hossiany and A. E. S. Fouda. Novel pyrimidine-bichalcophene derivatives as corrosion inhibitors for copper in 1 M nitric acid solution. Scientific Reports.2021; 11: 25314.

15. Mohammed O, Mohamed R, Driss T, Youssef N, Awad AA, Hassane L. Elucidating the role of novel halogenated hydroquinazolinone derivatives in mitigating copper corrosion in saline conditions: A joint assessment of experimental outcomes and computational analysis Journal of Molecular Liquids. 2023; 390: 122966.

16. Mohammed O, Mohamed R, Hassane L, Driss T, Youssef N, Awad AA, Han-seung L. Exploring sustainable corrosion inhibition of copper in saline environment: An examination of hydroquinazolinones via experimental and ab initio DFT simulations. Arabian Journal of Chemistry. 2024; 17(5): 105716.

17 Tigori MA, Koné A, Souleymane B, Zon D, Sissouma D, Niamien, PM Combining Experimental and Quantum Chemical Study of 2-(5-Nitro-1,3-Dihydro Benzimi-dazol-2-Ylidene)-3-Oxo-3-(2-Oxo-2HChromen-3-yl) Propanenitrile as Copper Corrosion Inhibitor in Nitric Acid Solution. Open Journal of Physical Chemistry. 2022; 12, 47-70.

18.Venkatesan H, Maya KP, Subramanian C, Manoharan S, Seung-Hyun K, Ill-Min Utilization of biowaste as an eco-friendly biodegradable corrosion inhibitor for mild steel in 1 mol/L HCl solution. Arabian Journal of Chemistry. 2020; 13(12): 8684-8696.

19. Venkatesan H, Ill-Min C, Seung-Hyun K, Mayakrishnan P. Inhibitory effect of biowaste on copper corrosion in 1 M HCl solution. Materials Today Communications. 2021, 27: 102249.

20. Frisch MJ, Trucks GW, Schlegel HB, Scuseria GE, Robb, MA, Cheeseman JR, et *al*. Gaussian 09. Gaussian, Inc., Wallingford, CT; 2009.

21 Becke D. Density functional calculations of molecular bond energies. The Journal of Chemical Physics. 1986; 84: 4524-4529.

22 Lee C, Yang W, Parr RG. Development of the correlation-energy formula into a functional of the electron density. Physical Review B. 1988; 37: 785.

23. Gadow HS, Thoraya AF, Eldesoky A.M. Experimental and theoretical investigations for some spiropyrazoles derivatives as corrosion inhibitors for copper in 2 M HNO_3 solutions. Journal of Molecular Liquids. 2019; 294: 111614.

24. Shalabi K, Ebrahim AG, El-Askalany AH, Abdallah, YM. Adsorption, Electrochemical Behavior, and Theoretical Studies for Copper Corrosion Inhibition in 1 M Nitric acid Medium using Triazine Derivatives. Journal of Molecular Liquids. 2022, 348: 118420.

25. Hamid A, Mohamed E, Aisha HA, Ehteram AN, Abdallah H, Ali D, Lahcen B, M'hamed B, Rachid S, Maryam C, Abdelkarim C, Young GK. From nature to protection: Unleashing the protective potential of Hedera helix leaves against corrosion in harsh acidic environments using experimental and theoretical insights. Arabian Journal of Chemistry.2024; 17(2): 105593.

26. Ehteram AN, Aisha HA. Thermodynamic study of metal corrosion and inhibitor adsorption processes in mild steel/1-methyl-4[4′(-X)-styryl pyridinium iodides/hydrochloric acid systems. Materials Chemistry and Physics.2008; 110(1):145-154.

27. Zarrouk A, Warad I, Hammouti B, Dafali A, Al-Deyab SS, Benchat N. The Effect of Temperature on the Corrosion of Cu/HNO_3 in the Presence of Organic Inhibitor: Part-2. International Journal of Electrochemical Science. 2010; 5: 1516 – 1526).

28. Issaadi S, Douadi SC. Adsorption and inhibitive properties of a new heterocyclic furan Schiff base on corrosion of copper in HCl 1M: Experimental and theoretical investigation .Applied Surface Science, 2014; 316: 582-589.

29. Yue X., Shengtao Z., Wenpo L., Lei G., Shenying X., Li F., Loutfy HM. Experimental and theoretical investigations of some pyrazolo-pyrimidine derivatives as corrosion inhibitors on copper in sulfuric acid solution. Applied Surface Science, 2018; 459: 612-620.

30. Gerengi H, Mielniczek M, Gece G, Solomon MM. Experimental and Quantum Chemical Evaluation of 8-Hydroxyquinoline as a Corrosion Inhibitor for Copper in 0.1 M HCl. Industrial & Engineering Chemistry Research. 2016; 55: 9614-9624.

31. Issaadi S, Douadi T, Chafaa S. Adsorption and inhibitive properties of a new heterocyclic furan Schiff base on corrosion of copper in HCl 1M: Experimental and theoretical investigation. Applied Surface Science. 2014; 316: 582-589.

32. Abdallah M, Al Bahira A, Altass HM, Fawzy A, El Guesmi N, Al-Gorair AS, Warad FB, Zarrouk A. Anticorrosion and Adsorption Performance of Expired Antibacterial Drugs on Sabic Iron Corrosion in HCl Solution: Chemical, Electrochemical and Theoretical Approach. Journal of Molecular Liquids.2021; 330: 115702.

33. K Vranda KS, Pushyaraga PV, Reena Kumari PD, Debashree C. Effective inhibition of mild steel corrosion by 6-bromo-(2,4-dimethoxyphenyl)methylidene]imidazo [1,2-

a]pyridine-2-carbohydrazide in 0.5 M HCl: Insights from experimental and computational study. Journal of Molecular Structure. 2021; 1232: 130074.

34. Abdallah EA, Aaziz J, Moutie MR, Rachid O, Khalid A, Hanane Z, Mustapha H, Hassan B, Lahcen B, Souad El I. Computational and experimental studies of the inhibitory effect of imidazole derivatives for the corrosion of copper in an acid medium. Journal of Molecular Liquids. 2022; 345: 117813.

35. Dheeraj S C, Chandrabhan V, Quraishi MA. Molecular structural aspects of organic corrosion inhibitors: Experimental and computational insights. Journal of Molecular Structure. 2021; 1227:129374**.**

36. Lei G., Ime Bassey O., Xingwen Z, Xun S, Yujie Q, Savaş K, Cemal .Theoretical insight into an empirical rule about organic corrosion inhibitors containing nitrogen, oxygen, and sulfur atoms. Applied Surface Science.2017; 406, 301-306.

37. Rajesh H, Dwarika P, Akhil S, Raman K. Experimental and theoretical studies of Ficus religiosa as green corrosion inhibitor for mild steel in 0.5 M H_2SO_4 solution. Sustainable Chemistry and Pharmacy.2018; 9: 95-105.

38. Sourav KS, Pritam G, Abhiram H, Naresh CM, Priyabrata B. Density functional theory and molecular dynamics simulation study on corrosion inhibition performance of mild steel by mercapto-quinoline Schiff base corrosion inhibitor. Physica E: Low-dimensional Systems and Nanostructures. 2015; 66:332-341.

39. Tengda M, Baimei T, Lei G, Savaş K, Zhengxiao K, Shihao Z, Ru W, Nengyuan Z, Yangang H. Multidimensional insights into the corrosion inhibition of potassium oleate on Cu in alkaline medium: A combined Experimental and theoretical investigation. Materials Science and Engineering.2021; 272: 115330.

40. Michaelson H.B. The Work Function of the Elements and Its Periodicity. Journal of Applied Physics. 1977; 48: 4729-4733.

41. Lukman OO, Mwadham MK, Eno EE. Quinoxaline derivatives as corrosion inhibitors for mild steel in hydrochloric acid medium: Electrochemical and quantum chemical studies. Physica E: Low-dimensional Systems and Nanostructures. 2016; 76: 109-126.

42. Gazquez JL,Cedillo A, Vela A. Electrodonating and electroaccepting powers.The Journal of Physical Chemistry. 2007; 111: 1966- 1970.

43. Rbaa M, Benhiba F, Obot IB, Oudda H, Warad I, Lakhrissi B, Zarrouk A. Two new 8-hydroxyquinoline derivatives as an efficient corrosion inhibitors for mild steel in hydrochloric acid: Synthesis, electrochemical, surface morphological, UV–visible and theoretical studies. Journal of Molecular Liquids. 2019, 276, 15:120-133.

44. Hassane L, Rachid S, Shehdeh J, Belkheir H. Effect of clozapine on inhibition of mild steel corrosion in 1.0 M HCl medium, Journal of Molecular Liquids Journal of Molecular Liquids.2017; 225:271-280

45. Morell CA, Toro-Labbé A. New Dual Descriptor for Chemical Reactivity. Journal of Physical Chemistry A. 2005; 109: 205-212.

46. Martínez.A.JI. (2015). Why Is the Dual Descriptor a More Accurate Local Reactivity Descriptor than Fukui Functions? Journal of Mathematical Chemistry, 5: 451-465.

47. Hualiang H, Xiaomeng G.The relationship between the inhibition performances of three benzo derivatives and their structures on the corrosion of copper in 3.5 wt.% NaCl solution. Colloids and Surfaces A: Physicochemical and Engineering Aspects. 2020; Volume 598: 124809.